Int. J. Sci. R. Tech., 2026 3(5)
A Multidisciplinary peer-reviewed Journal
www.ijsrtjournal.com [ISSN: 2394-7063]

Original Article

Design And Synthesis Of Sulfonamides Containing New Pteridine Analogues For The Management Of Rheumatoid Arthritis

Nitypal Singh Chouhan*[1], Hemant Badwaik[2]

[1]*Shri Rawatpura Sarkar Institute of Pharmacy, Near Power Grid, Kumhari, Durg Chhattisgarh 490042, India.*
[2]*Shri Shankaracharya Institute of Pharmaceutical Sciences and Research, SSPU, Bhilai, Chhattisgarh 490020, India.*

ABSTRACT

Objective: This study involved the Design and synthesis of novel pteridine derivatives linked to sulfonamide molecules (5a-f) and their study of antioxidant, antiarthritic activity, and molecular docking capability towards the rheumatoid arthritis (RA) associated targets. Materials and Methods: The synthesis of the target compounds involved a multiple-step synthetic procedure and was characterized by FT-IR, 1D NMR (1H NMR and 13C NMR), and mass spectroscopy. Antioxidant activity was measured using the DPPH free radical scavenging assay, and antiarthritic activity was determined by the Complete Freund's Adjuvant (CFA) induced arthritis in Wistar rats by assessing oedema of the paws for 28 days. Molegro Virtual Docker was used to perform molecular docking studies against the human dihydroorotate dehydrogenase complexed with antiproliferative agent (PDB: 1D3H) to assess molecular interaction patterns and binding affinity. Results and Discussion: The synthesized derivatives were found to yield good yields (82-86%) and maintained the structural integrity of the derivatives when analyzed by spectral characterization. However, compound 5b had the most potent antioxidant activity among all the compounds, with an IC50 value of 28.77 ± 0.86 µg/mL, which was higher than that of ascorbic acid. In the evaluation of antiarthritic activity, compound 5b exhibited a strong antiarthritic activity response with a maximum paw oedema inhibition of −43.68% on day 28. Its activity was also corroborated using molecular docking analysis, where compound 5b possessed the highest binding affinity (MolDock score: -193.269 kcal/mol) with favorable hydrogen bonding interactions with critical amino acids such as Thr212, Asn382, and His388. Conclusion: These findings indicate that compound 5b, with high antioxidant and antiarthritic efficacy and significant molecular interactions, could be a potential lead compound for developing novel drug molecules for RA.

Keywords: rheumatoid arthritis (RA), Wistar rats, Antioxidant, antiarthritic efficacy, chronic inflammation.

INTRODUCTION

Rheumatoid arthritis (RA) is a chronic progressive and systemic autoimmune inflammatory disorder in which progressive synovial inflammation, the formation of pannus, cartilage degradation, and irreversible bone erosion all lead to progressive joint deformity and functional disability [1]. In RA, the immune system infiltrates tissues that are found in a joint. These activated cells over-express pro-inflammatory cytokines (including tumor necrosis factor-α (TNF-α), interleukin (IL)-1, IL-6, IL-17, and matrix metalloproteinases (MMPs)), which are thought to be associated with chronic inflammation and progressive loss of cartilage and bone [2]. In addition, inflammatory mediators, such as prostaglandins (PGs), leukotrienes (LTs), nitric oxide (NO), platelet-activating factor (PAF), and reactive oxygen species (ROS) contribute to the enhancement of oxidative stress and inflammatory response in RA. Evidence is emerging that oxidative stress plays a significant role in the progression of disease by promoting tissue damage and the production of cytokines [3]. Pharmacological treatment for RA currently includes non-steroidal anti-inflammatory drugs (NSAIDs), corticosteroids, disease-modifying antirheumatic drugs (DMARDs), and biological

Relevant conflicts of interest/financial disclosures: The authors declare that the research was conducted in the absence of any commercial or financial relationships that could be construed as a potential conflict of interest.

agents, which relieve RA symptoms but may also have side effects, resistance, toxicity, and unknown long-term safety. Hence, there is a great need for the discovery of new small molecules that can have anti-inflammatory, antioxidant, and immunomodulatory properties that are more effective and less toxic than the existing formulations. Dihydroorotate dehydrogenase (DHODH) is one of the emerging targets for drugs to treat RA. DHODH is a mitochondria-bound enzyme that catalyzes the oxidation of dihydroorotate (DHO) to orotate, which is a crucial and rate-limiting part of de novo pyrimidine biosynthesis. It is instrumental in the quick proliferation of activated lymphocytes, so blocking DHODH can inhibit the proliferation of activated lymphocytes and inflammation. DHODH has been reported as a promising molecular target in RA therapy since clinically used DHODH inhibitors like leflunomide are effective. Another target of autoimmune diseases of importance is dihydrofolate reductase (DHFR), which is an essential enzyme in folate metabolism and in thymidylate and purine biosynthesis for DNA replication and cell proliferation [5]. Inhibition of DHFR is an event that disrupts the biosynthesis of nucleotides and can lead to less proliferation of activated immune cells. The activity of methotrexate, a commonly used DMARD drug for RA, is mainly mediated through its action on DHFR. Therefore, new molecules that interact with DHODH and DHFR have potential for providing new therapeutic leads for RA [6]. The pteridine derivatives are important heterocyclic bioactive compounds with varied biological activities like anti-inflammatory, anti-oxidant, anti-microbial, anti-tumoral, and immune modulator [7]. Pteridine scaffolds share interesting structural features with folate analogues and are suitable HIV drug targets. Moreover, it is interesting that the incorporation of amino-substituted pteridine moieties could be beneficial in facilitating interaction with inflammatory and proliferative signaling pathways involved in RA. The present study was aimed to design and synthesize novel pteridine analogues for the evaluation of anti-rheumatoid activity, based on the above-mentioned observations. The synthesized compounds were characterized by the use of suitable physicochemical and spectral methods. They were used for assessing the antioxidant activity to assess the free radical scavenging potential, as high oxidative stress has been involved in the progression of RA. Moreover, the synthesized compounds were tested for their antiarthritic activity with proper *in vitro* and *in vivo* models in order to evaluate their anti-inflammatory effect. In order to illustrate the possible mechanisms of action and binding affinities towards various important therapeutic targets, a molecular docking study was carried out with DHODH and DHFR, which are associated with RA. The joint experimental and computational strategy can be used to help identify interesting pteridine derivatives that might be useful in the treatment of rheumatoid arthritis. Thus, in the present work, attempts are made to design, synthesize, evaluate their biological activity, screen for antioxidant activity, assess their anti-arthritic activity, and elucidate the possible mechanism using a molecular docking approach to develop potential therapeutic candidates in the context of rheumatoid arthritis.

2. MATERIALS AND METHODS

2.1 Materials and Equipment

All the chemicals and the constituents used here in the present study were obtained from Alpha Chemika, 2022-2023, Andheri W. Mumbai and Kasliwal brothers, Bhatia complex, Raipur. The melting points of the new-synthesized compounds were found by open capillary method and were uncorrected. Thin-layer chromatography (TLC) was used to follow the course of reactions and to determine the purity of synthesized compounds on Silica gel G (E. Merck) plates eluting with acetonitrile/carbon tetrachloride (60:40, v/v). The KBr pellet method was used to obtain infrared (IR) spectra by using the JASCO FTIR spectrophotometer. All the 1H NMR spectra were acquired in DMSO-d6 on a Bruker Advance 400 MHz NMR spectrophotometer with tetramethyl silane (TMS) as internal standard. The ^{13}C NMR spectra were obtained at 100 MHz in DMSO-d6. Mass spectral analysis was performed using electron ionization mass spectrometry (EI-MS) on a SHIMADZU-2010 AT mass spectrometer.

2.2 Synthesis and Characterization

2.2.1 General procedure for the synthesis of 2,6-diamino-5-nitrosopyrimidin-4-ol (1)

A mixture of guanidine hydrochloride (0.02 mol) and 50% aqueous NaOH solution was stirred, and 500 mL of ethyl cyanoacetate (0.02 mol) was slowly added to the reaction with stirring, with the reaction temperature raised under 40 °C. The reaction mixture was then slowly heated at a uniform speed on a bench-top using proper stirring, at 120-160 °C to the stage where water was no longer evolved and a whitish-brown precipitate was obtained. This was immediately cooled to below 100 °C, and the appropriate amount of water was added. The solution thus obtained was buffered by dropwise addition of concentrated HCl, and then an equimolar amount of sodium nitrite ($NaNO_2$) was added under continuous stirring, thus neutralized. Then, concentrated HCl was added dropwise into it until a deep pink-red precipitate was formed. The precipitate obtained was filtered, washed, dried, and recrystallized from ethanol to obtain the desired product [8].

Color: Deep pink-red powder; % Yield: 78-85%; M.P.: 164-172 °C; IR (KBr, cm^{-1}): 3420-3300 (O-H), 3180 (Ar C–H), 1665 (C=N), 1605 (N=O), 1560 (C=C), 1345 (C-N), 1240 (C-O), 1105 (N-O); ^{1}H NMR (400 MHz, DMSO-d_6) δ ppm: 5.40 (s, OH), 6.80-7.20 (NH_2), 8.10 (s, NH), 8.45 (s, heterocyclic proton); ^{13}C NMR (100 MHz, DMSO-d_6) δ ppm: 108.5, 126.4, 138.2, 145.6, 151.8, 156.4, 161.2.

2.2.2 General procedure for the synthesis of 2-amino-6-methyl-7-phenylpteridin-4-ol (2)

A solution of nitroso pyrimidine (0.02 mol) was prepared in DMSO using ultrasonication, followed by the addition of an equimolar alcoholic solution of potassium acetate under stirring. Subsequently, an equimolar amount of the propiophenone was dropwise added to the resulting mixture, which was refluxed for 3–4 h. Once the reaction was completed (checked by TLC), the mixture was allowed to cool and then diluted with 4% NaOH solution. The reaction mixture was neutralised with acetic acid and was poured on crushed ice, creating a precipitate. The solid obtained was filtered and washed, and then recrystallized from ethanol and dried, giving the desired compound [9].

Color: Light pink rose powder; % Yield: 82.40; M.P.: 238–242 °C; IR (KBr, cm^{-1}): 3418.62 (O-H), 3328.45 (N-H), 3058.73 (Ar C-H), 2924.38 (CH_3), 1662.84 (C=O/OH tautomeric), 1615.27 (C=N), 1568.14 (Ar C=C), 1328.56 (C–N); ^{1}H NMR (400 MHz, DMSO-d_6) δ ppm: 2.31 (s, 3H, CH_3), 7.12–7.58 (m, 5H, Ar-H), 8.05 (s, 1H, NH), 8.62 (s, 1H, NH), 10.84 (s, 1H, OH); ^{13}C NMR (100 MHz, DMSO-d_6) δ ppm: 18.6, 116.8, 123.5, 126.2, 128.4, 130.7, 136.9, 145.2, 151.8, 156.4, 160.7, 164.3;

2.2.3 General procedure for the synthesis of 3,4,5-trihydroxy-N-(4-hydroxy-6-methyl-7-phenylpteridin-2-yl) benzamide (3)

The equimolar solution of Intermediate 2, along with boric acid and gallic acid were refluxed for 16 h in ethanol. TLC was used for monitoring the progress of the reaction. Once the reaction was completed, the reaction mixture was cooled to room temperature, and then n-hexane was added to the mixture. This mixture was then poured onto crushed ice, and a precipitate was formed. The solid obtained was collected, washed with cold water, and recrystallized from ethanol, filtered, and dried at 50-60 °C to yield the final compound [10].

Color: Brownish yellow powder; % Yield: 79.65; M.P.: 262-267 °C; IR (KBr, cm^{-1}): 3435.84 (O-H), 3322.71 (N-H), 3065.48 (Ar C-H), 2931.62 (CH_3), 1712.45 (C=O, amide), 1658.73 (C=N), 1608.26 (Ar C=C), 1542.81 (N-H bending), 1368.35 (C-N), 1246.74 (phenolic C-O); ^{1}H NMR (400 MHz, DMSO-d_6) δ ppm: 2.28 (s, 3H, CH_3), 6.15-6.82 (m, 3H, aromatic OH-substituted ring), 7.10-7.64 (m, 5H, Ar-H), 8.18 (s, 1H, NH), 8.74 (s, 1H, NH), 9.45-10.26 (s, 3H, OH), 11.12 (s, 1H, CONH); ^{13}C NMR (100 MHz, DMSO-d_6) δ ppm: 18.9, 102.8, 108.6, 114.2, 118.5, 123.8, 126.4, 128.1, 130.6, 136.8, 145.3, 148.6, 151.2, 156.7, 160.4, 164.8, 169.5;

2.2.4 General procedure for the synthesis of 4-(4-hydroxy-6-methyl-2-(3,4,5-trihydroxybenzamido) pteridin-7-yl) benzene sulfonyl chloride (4)

An equimolar solution of Intermediate 3 was prepared in glacial acetic acid, and Zinc chloride (ZnCl2) was added to the prepared equimolar solution and stirred continuously. A viscous red solution was formed by heating the reaction mixture at 142 °C for 1-2 h. The reaction was completed by TLC, and then the mixture was cooled to room temperature. The solution, which was cooled, was stirred continuously, and the aqueous HCl solution (saturated aqueous HCl: water, 1/1 v/v) was added dropwise so that a precipitate was formed.

The obtained solid was filtered, washed with distilled water, and dried to yield the desired product [11].

Color: White powder; % Yield: 81.72; M.P.: 212-216 °C; IR (KBr, cm^{-1}): 3442.36 (O-H), 3335.84 (N-H), 3062.18 (Ar C-H), 2928.47 (CH_3), 1710.65 (C=O, amide), 1652.84 (C=N), 1604.72 (Ar C=C), 1546.18 (N-H), 1378.35 (S=O, sulfonyl), 1324.67 (C-N), 1242.56 (phenolic C-O), 1168.48 (S=O asymmetric stretching), 758.31 (S-Cl); ^{1}H NMR (400 MHz, DMSO-d_6) δ ppm: 2.34 (s, 3H, CH_3), 6.22-6.88 (m, 3H, aromatic OH-substituted ring), 7.18-7.95 (m, 4H, Ar-H), 8.24 (s, 1H, NH), 8.82 (s, 1H, NH), 9.58-10.38 (s, 3H, OH), 11.26 (s, 1H, CONH); ^{13}C NMR (100 MHz, DMSO-d_6) δ ppm: 18.7, 103.2, 108.4, 114.8, 119.2, 124.6, 127.3, 129.8, 133.6, 138.2, 145.8, 149.4, 152.1, 156.8, 160.6, 165.2, 170.1.

2.2.5 General procedure for the synthesis of 3,4,5-trihydroxy-N-(4-hydroxy-6-methyl-7-(4-(N-(substituted) sulfamoyl) phenyl) pteridin-2-yl) benzamide (5a-f)

An equimolar amount of substituted aniline derivative was then added to a solution of the intermediate compound (0.001mol) in ethanol, while stirring, which resulted in a solution of product 2 (0.001mol). Then, an aqueous solution at 0-5 ° C of NaOH 2% was dropped into the reaction mixture. The reaction was stirred continuously till appearance of a yellowish-brown precipitate occurred at the same temperature for 2-3 h, and the reaction progress was monitored by using TLC. The precipitate thus obtained was filtered, washed with cold ethanol, and recrystallized from ethanol. The purified product was finally dried at 50-60 °C to yield the desired product [12].

2.2.6 3,4,5-trihydroxy-N-(4-hydroxy-6-methyl-7-(4-(N-(o-tolyl) sulfamoyl) phenyl) pteridin-2-yl) benzamide (5a)

Color: yellowish-brown powder; % Yield: 84.18; M.P.: 241-246 °C; IR (KBr, cm^{-1}): 3448.52 (O-H), 3332.84 (N-H), 3068.27 (Ar C-H), 2934.62 (CH_3), 1708.46 (C=O, amide), 1655.28 (C=N), 1606.74 (Ar C=C), 1544.38 (N-H), 1365.82 and 1162.47 (SO_2, sulfonamide stretching), 1328.65 (C-N), 1244.58 (phenolic C-O); ^{1}H NMR (400 MHz, DMSO-d_6) δ ppm: 2.26 (s, 3H, CH_3), 2.38 (s, 3H, Ar-CH_3), 6.18-6.85 (m, 3H, aromatic OH-substituted ring), 7.02-7.88 (m, 8H, Ar-H), 8.16 (s, 1H, NH), 8.76 (s, 1H, NH), 9.42-10.28 (s, 3H, OH), 10.84 (s, 1H, SO_2NH), 11.18 (s, 1H, CONH); ^{13}C NMR (100 MHz, DMSO-d_6) δ ppm: 18.8, 21.4, 102.6, 108.8, 114.6, 118.4, 123.7, 126.2, 128.5, 130.8, 133.2, 136.9, 142.8, 145.6, 149.2, 152.4, 156.5, 160.2, 164.8, 169.7; MS: calculated [M^+] m/z Found: 574.08.

2.2.7 3,4,5-trihydroxy-N-(4-hydroxy-7-(4-(N-(3-methoxyphenyl) sulfamoyl) phenyl)-6-methylpteridin-2-yl) benzamide (5b)

Color: bright yellow powder; % Yield: 85.36; M.P.: 229-234 °C; IR (KBr, cm^{-1}): 3445.72 (O-H), 3336.48 (N-H), 3070.25 (Ar C-H), 2945.63 (CH_3), 1712.36 (C=O, amide), 1654.82 (C=N), 1608.45 (Ar C=C), 1546.38 (N-H), 1368.54 and 1165.22 (SO_2 asymmetric and symmetric stretching), 1325.84 (C-N), 1252.73 (Ar-O-CH_3), 1238.46 (phenolic C-O); ^{1}H NMR (400 MHz, DMSO-d_6) δ ppm: 2.28 (s, 3H, CH_3), 3.76 (s, 3H, OCH_3), 6.15-6.82 (m, 3H, aromatic OH-substituted ring), 6.95-7.92 (m, 8H, Ar-H), 8.18 (s, 1H, NH), 8.74 (s, 1H, NH), 9.48-10.34 (s, 3H, OH), 10.88 (s, 1H, SO_2NH), 11.24 (s, 1H, CONH); ^{13}C NMR (100 MHz, DMSO-d_6) δ ppm: 18.6, 55.4, 102.8, 108.5, 114.2, 116.4, 119.3, 123.8, 126.7, 128.6, 130.4, 133.5, 138.2, 145.4, 149.6, 152.3, 156.8, 159.4, 160.7, 164.9, 169.8; MS: calculated [M^+] m/z Found: 590.02.

2.2.8 3,4,5-trihydroxy-N-(4-hydroxy-6-methyl-7-(4-(N-(4-nitrophenyl) sulfamoyl) phenyl) pteridin-2-yl) benzamide (5c)

Color: Dark yellow powder; % Yield: 83.84; M.P.: 221-225 °C; IR (KBr, cm^{-1}): 3442.68 (O-H), 3334.25 (N-H), 3072.16 (Ar C-H), 2932.74 (CH_3), 1710.42 (C=O, amide), 1656.38 (C=N), 1605.84 (Ar C=C), 1532.48 (NO_2 asymmetric stretching), 1544.72 (N-H bending), 1364.28 (SO_2 stretching), 1346.15 (NO_2 symmetric stretching), 1162.54 (SO_2 symmetric stretching), 1240.62 (phenolic C–O), 1328.47 (C-N); ^{1}H NMR (400 MHz, DMSO-d_6) δ ppm: 2.30 (s, 3H, CH_3), 6.18-6.86 (m, 3H, aromatic OH-substituted ring), 7.18-8.24 (m, 8H, Ar-H), 8.28 (s, 1H, NH), 8.82 (s, 1H, NH), 9.52-10.38 (s, 3H, OH), 10.92 (s, 1H, SO_2NH), 11.30 (s, 1H, CONH); ^{13}C NMR (100 MHz, DMSO-d_6) δ ppm: 18.8, 102.6, 108.9, 114.4, 119.2, 123.8, 125.6, 127.4, 130.8, 136.4, 142.8, 145.7, 147.6, 149.8, 152.5, 156.6, 160.5, 164.8, 169.9; MS: calculated [M^+] m/z Found: 605.02.

2.2.9 N-(7-(4-(N-(2-chlorophenyl) sulfamoyl) phenyl)-4-hydroxy-6-methylpteridin-2-yl)-3,4,5-trihydroxybenzamide (5d)

Color: yellow powder; % Yield: 84.62; M.P.: 238-242 °C; IR (KBr, cm^{-1}): 3446.38 (O-H), 3331.54 (N-H), 3068.72 (Ar C-H), 2934.18 (CH_3), 1711.26 (C=O, amide), 1654.84 (C=N), 1607.48 (ArC=C), 1542.65 (N-H), 1366.84 and 1164.52 (SO_2 asymmetric and symmetric stretching), 1324.36 (C-N), 1242.58 (phenolic C-O), 758.42 (C-Cl); ^{1}H NMR (400 MHz, DMSO-d_6) δ ppm: 2.29 (s, 3H, CH_3), 6.16-6.84 (m, 3H, aromatic OH-substituted ring), 7.08-7.96 (m, 8H, Ar-H), 8.22 (s, 1H, NH), 8.78 (s, 1H, NH), 9.46-10.32 (s, 3H, OH), 10.86 (s, 1H, SO_2NH), 11.22 (s, 1H, CONH); ^{13}C NMR (100 MHz, DMSO-d_6) δ ppm: 18.7, 102.8, 108.6, 114.5, 118.8, 123.6, 126.8, 128.4, 130.6, 132.8, 136.9, 142.6, 145.5, 149.4, 152.2, 156.7, 160.4, 164.9, 169.8; MS: calculated [M^+] m/z Found: 594.01.

2.2.10 N-(7-(4-(N-(4-bromophenyl) sulfamoyl) phenyl)-4-hydroxy-6-methylpteridin-2-yl)-3,4,5-trihydroxybenzamide (5e)

Color: Brown powder; % Yield: 82.94; M.P.: 211-216 °C; IR (KBr, cm^{-1}): 3444.52 (O-H), 3333.68 (N-H), 3066.84 (Ar C-H), 2932.45 (CH_3), 1710.84 (C=O, amide), 1655.26 (C=N), 1606.52 (Ar C=C), 1543.28 (N-H), 1367.46 and 1163.82 (SO_2 asymmetric and symmetric stretching), 1326.24 (C-N), 1241.58 (phenolic C-O), 612.34 (C-Br); ^{1}H NMR (400 MHz, DMSO-d_6) δ ppm: 2.31 (s, 3H, CH_3), 6.18-6.86 (m, 3H, aromatic OH-substituted ring), 7.12-8.02 (m, 8H, Ar-H), 8.24 (s, 1H, NH), 8.80 (s, 1H, NH), 9.48-10.34 (s, 3H, OH), 10.88 (s, 1H, SO_2NH), 11.26 (s, 1H, CONH); ^{13}C NMR (100 MHz, DMSO-d_6) δ ppm: 18.8, 102.7, 108.8, 114.6, 119.1, 123.8, 126.6, 128.8, 130.7, 132.4, 137.2, 142.8, 145.6, 149.5, 152.3, 156.8, 160.5, 165.1, 169.9; MS: calculated [M^+] m/z Found: 637.58.

2.2.11 N-(7-(4-(N-(4-ethylphenyl) sulfamoyl) phenyl)-4-hydroxy-6-methylpteridin-2-yl)-3,4,5-trihydroxybenzamide (5f)

Color: Off-white powder; % Yield: 85.74; M.P.: 232-236 °C; IR (KBr, cm^{-1}): 3448.26 (O-H), 3334.72 (N-H), 3068.45 (Ar C-H), 2962.84 and 2931.42 (aliphatic C-H), 1712.34 (C=O, amide), 1654.68 (C=N), 1605.82 (Ar C=C), 1543.28 (N-H), 1368.56 and 1164.22 (SO_2 asymmetric and symmetric stretching), 1325.64 (C-N), 1240.85 (phenolic C-O); ^{1}H NMR (400 MHz, DMSO-d_6) δ ppm: 1.18 (t, 3H, CH_3), 2.58 (q, 2H, CH_2), 2.30 (s, 3H, heterocyclic CH_3), 6.16-6.84 (m, 3H, aromatic OH-substituted ring), 7.02-7.92 (m, 8H, Ar-H), 8.20 (s, 1H, NH), 8.76 (s, 1H, NH), 9.46-10.28 (s, 3H, OH), 10.84 (s, 1H, SO_2NH), 11.18 (s, 1H, CONH); ^{13}C NMR (100 MHz, DMSO-d_6) δ ppm: 15.2, 18.7, 28.4, 102.8, 108.5, 114.6, 118.8, 123.7, 126.4, 128.6, 130.8, 136.8, 142.6, 145.5, 149.4, 152.2, 156.7, 160.4, 164.8, 169.7; MS: calculated [M^+] m/z Found: 588.05.

2.3 Biological Activity

2.3.1 Antioxidant Activity

The antioxidant activity of the synthesized compound was evaluated using the 2,2-diphenyl-1-picrylhydrazyl (DPPH) free radical scavenging assay. A 0.1 mM methanolic DPPH solution was prepared and mixed with different concentrations of the test compound (20, 40, 60, 80, and 100 µg/mL). The reaction mixtures were incubated in the dark at room temperature for 30 min to allow completion of the reaction. After incubation, absorbance was measured at 517 nm using a UV–Visible spectrophotometer against methanol as the blank. The decrease in absorbance relative to the DPPH control was considered indicative of radical scavenging activity, and the percentage inhibition was calculated accordingly [13].

2.3.2 Experimental Animals

Albino Wistar Rats of either sex (150–200 g, 15–18 weeks old) were used for the in vivo study. Animals were procured from the Central Animal Facility of Shri Rawatpura Sarkar Institute of Pharmacy and acclimatized under standard laboratory conditions, including a temperature of 25 ± 2 °C, relative humidity of 60-70%, and a 12 h light/dark cycle. The animals were housed in polypropylene cages with free access to standard pellet feed and water throughout the study period. All experimental protocols were performed in accordance with the guidelines established by the Committee for Control and Supervision of Experiments on Animals (CCSEA). Ethical approval for conducting the study was obtained from the Institutional Animal Ethics Committee (IAEC), Shri Rawatpura Sarkar Institute

of Pharmacy (Approval No.: SRIP/IAEC/2024/25/B/11).

2.3.3 *In-vivo* Anti-arthritic Activity

Inflammation and arthritic potential were evaluated in the Complete Freund's Adjuvant (CFA)-induced arthritis model. Rats were divided into four groups (n=6). Groups II through IV were given only a single CFA injection (0.1 mL) into the left hind paw and Group I was injected with saline. Once a day for 28 days, the topical applications (Placebo, Lefluonamide, compound 5b) were applied after the induction. Paw edema was assessed on days 0, 7, 14, 21 and 28 to evaluate the course of the disease and the therapeutic response.[14].

2.4 Computational Study

2.4.1 Molecular Docking Study

Molecular docking analysis was performed to evaluate the binding affinity, interaction patterns, and molecular recognition of the synthesized quinazoline derivatives (5a-f) and the standard drug Leflunomide against the human dihydroorotate dehydrogenase complexed with antiproliferative agent (PDB: 1D3H, Resolution: 1.80 Å). The crystal structure of the target protein was retrieved from the Protein Data Bank (PDB) database [15-16]. The two-dimensional (2D) chemical structures of the synthesized compounds and standard drug were drawn using ChemDraw version 22.2.0 (64-bit) and subsequently converted into three-dimensional (3D) molecular geometries using Chem3D version 22.2.0 (64-bit). The generated 3D structures were subjected to energy minimization using the MM2 force field algorithm to obtain stable conformations with minimum energy. The optimized ligand structures were exported in pdb format for further docking analysis [17]. Molecular docking simulations were carried out using Molegro Virtual Docker (MVD) version 6.0. The docking protocol was performed within the active site cavity of the target protein by defining the binding pocket parameters, including cavity surface area and volume. A spherical search space with a radius of 15.0 Å was employed around the active binding region. Docking calculations were conducted using a grid resolution of 0.30 Å, population size of 50, 1500 iterations, and 10 independent runs per ligand to ensure optimal binding conformations [18-19]. The binding interactions, docking poses, hydrogen bonding, steric interactions, and ligand–protein interaction profiles of the docked complexes were further visualized and analyzed using Discovery Studio Visualizer (BIOVIA). The docking results were interpreted based on binding energy scores, interaction patterns, and molecular stability within the active site of the target protein [20].

3. RESULTS AND DISCUSSION

3.1 Chemistry

The synthetic pathway adopted for the preparation of target sulfonamide-linked pteridine derivatives (5a-f) involved a multistep reaction sequence as illustrated in Scheme 1. Reaction of guanidine hydrochloride and ethyl cyanoacetate, first in alkaline conditions such as sodium hydroxide, yielded the expected condensation product, 2,6-diamino-5-nitrosopyrimidin-4-ol (1). The characteristic bands in the IR spectrum for the nitrosite group, imine group, and hydroxyl group confirmed the formation of compound 1. The ^{1}H NMR spectrum revealed the signals of NH_2, NH, and hydroxyl protons, and the peaks in the ^{13}C NMR spectrum confirmed the pyrimidine structure. Treatment of intermediate 1 with propiophenone containing potassium acetate resulted in cyclization to yield 2-amino-6-methyl-7-phenylpteridin-4-ol (2). The presence of a characteristic 2 protons resonating at a chemical shift of δ 2.31 ppm in the ^{1}H NMR spectrum is indicative of successful formation of the pteridine nucleus, with the corresponding disappearance of nitroso-related peaks demonstrating the successful incorporation of the 2-nitroso into ring. The aromatic proton resonances within the range of 7.12-7.58 ppm and the carbon resonance signal in the ^{13}C NMR also suggested the heterocyclic structure.

Compound 2 was coupled with gallic acid to give compound 3 as a 3,4,5-trihydroxy-N-(4-hydroxy-6-methyl-7-phenylpteridin-2-yl) benzamide. The introduction of the Amide moiety was confirmed by strong IR bands corresponding to C=O around 1712 cm^{-1} and broad bands corresponding to O-H stretching. Multiple hydroxyl proton signals (δ 9.45-10.26 ppm) and the amide NH proton resonance (δ 11.12 ppm) were visible in the ^1H NMR spectrum, verifying the formation of benzamide. Key intermediate 4 was obtained by functionalization of intermediate 3 with sulfonyl chloride. The

characteristic stretching vibration of sulfonyl groups is observed around 1378cm^{-1}, and the characteristic vibration of S-Cl appeared near 758cm^{-1}. The results supported the successful sulfonylation. Finally, intermediate 4 was subjected to nucleophilic substitution reactions with different substituted aniline derivatives to yield the desired sulfonamide derivatives (5a-f) in 82-86% yields. The synthetic compounds that were created had either more electron-donating or electron-withdrawing groups, such as a methyl group, a methoxy group, a nitro group, a chloro group, a bromo group, or an ethyl group. IR spectra of compounds (5a-f) in all cases showed absorption bands of the hydroxyl, aminocarbonyl, imine, and sulfonamide groups at 3442-3448, 1708-1712, 1654-1656, and 1364-1368, respectively, and 1162-1165 cm^{-1}, confirming the preservation of the core pharmacophore. The existence of a large amount of intermolecular hydrogen bonding was suggested by the presence of broad O-H and N-H stretching bands. All target compounds exhibited prominent singlets between 2.26 and 2.34 ppm in the 1H NMR spectrum, which corresponds to the pteridine methyl group. The protons in the aromatic rings occurred between δ 6.9-8.2 ppm, and the NH protons in sulfonamide groups appeared in the region of δ 10.84-10.92 ppm. The NH signals of the amides were observed downfield at δ 11.18-11.30 ppm, which was attributed to hydrogen bonding effects. The phenol hydroxyl protons were observed and found between δ 9.42-10.38 ppm, confirming the introduction of trihydroxy benzamide units. The ^{13}C NMR spectra also verified the structure of the synthetic derivatives by the presence of characteristic ^{13}C signals in the carbonyl region (δ 164-170 ppm) and aromatic/heterocyclic carbon region (δ 102-160 ppm). Other carbons confirmed the structure with a substituent C=O signal at 55.4 ppm in compound 5b, and C=O signals at 15.2 ppm and at 28.4 ppm in compound 5f. The molecular structures of compound (5a-f) were confirmed by means of mass spectral analysis, and the molecular ion peaks of the expected molecular weights (5a) m/z 574.08, (5b) m/z 590.02, (5c) m/z 605.02, (5d) m/z 594.01, (5e) m/z 637.58, and (5f) m/z 588.05 were observed. The molecular ion peaks were observed and correspond well with the calculated molecular weight values, indicating successful synthesis of the target compounds. In conclusion, the well-developed synthetic route was successfully employed for the synthesis of the desired sulfonamide-linked pteridines (5a-f) in moderate to excellent yields and with adequate methodological purity. All the synthesized compounds were characterized by the methods of spectroscopic data (FT-IR, ^{1}H NMR, ^{13}C NMR, and MS), which confirmed the proposed structures.

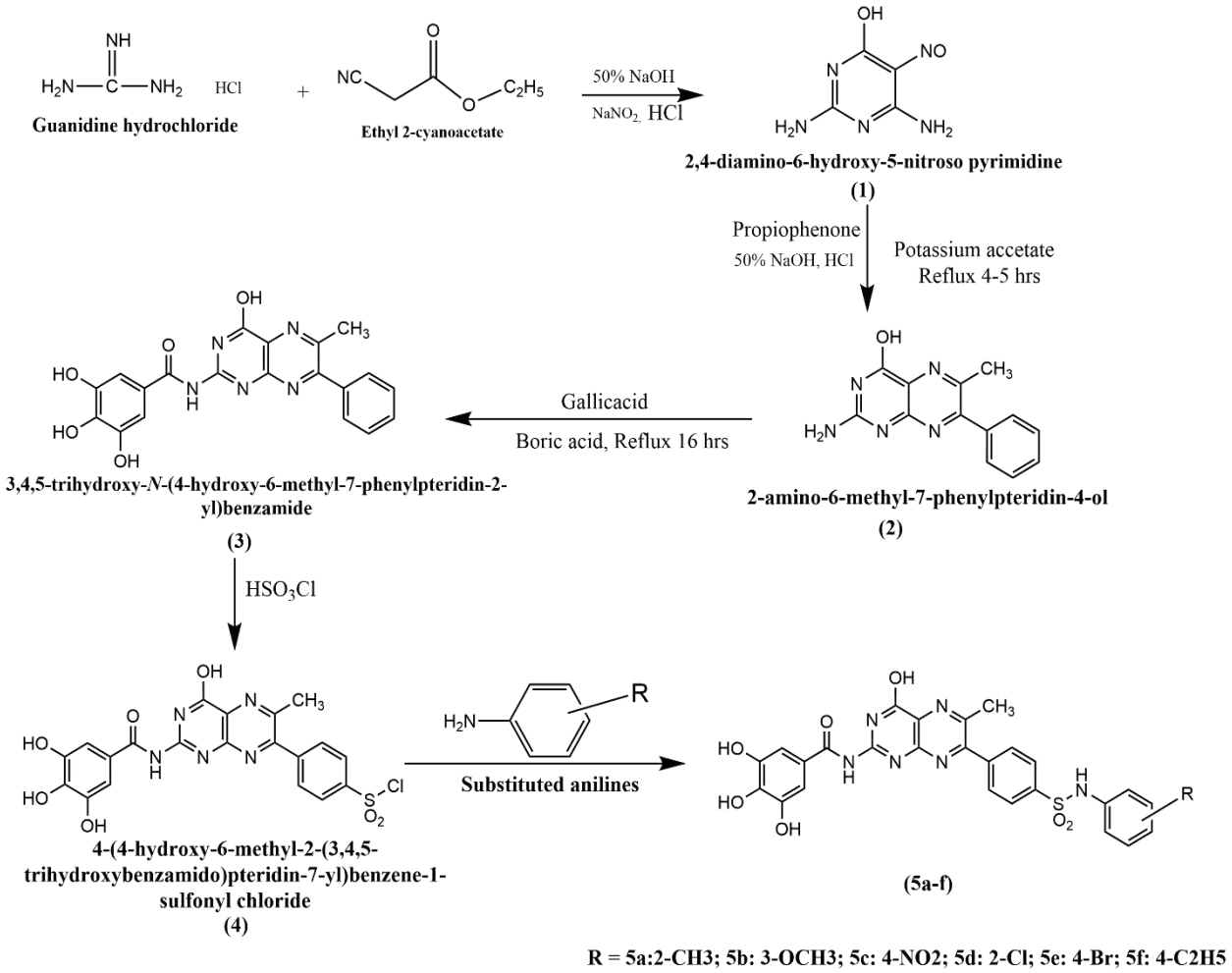

Scheme 1. Synthetic strategies for newly designed pteridine derivatives (5a-f).

3.2 Biological Activity

3.2.1 Antioxidant Activity

The antioxidant activity of the synthesized quinazoline derivatives (5a-f) was determined by DPPH free radical scavenging activity and compared to ascorbic acid (Figure 1). The analysis revealed that higher IC_{50} values were associated with higher antioxidant properties. The compound with the lowest IC_{50} value (28.77 ± 0.86 µg/mL) was compound 5b that has the highest antioxidant activity among all compounds tested, as compared to ascorbic acid (IC_{50} value = 33.67 ± 0.79 µg/mL). Compounds 5a, 5d, and 5e exhibited moderate antioxidant activity, whereas compounds 5c and 5f exhibited comparatively less, with a higher IC_{50} value. The increased activity of compound 5b can be explained by the effects of the 5b structure and substituents for the increased electron donation and radical stabilization. In summary, the results are indicative that compound 5b is the best antioxidant derivative of the synthesized compounds, and it can be used as a lead molecule for further biological studies.

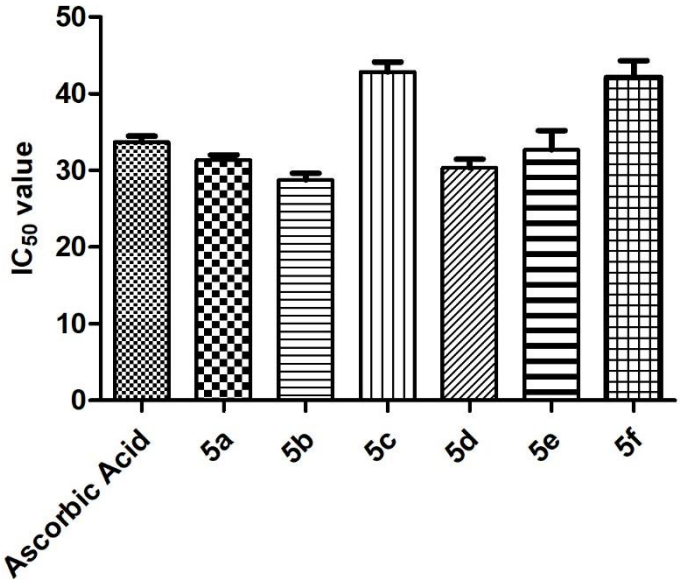

Figure 1. Antioxidant activity of the synthesized compounds (5a-f) along with ascorbic acid through DPPH assay.

3.2.2 Anti-arthritic Activity

The anti-arthritic activity of compound 5b was assessed by measuring the percent inhibition of paw oedema volume after 28 days and the results were compared with the control and standard-treated groups (Table 1). The increment of paw oedema was progressive in the control group over the study period, which is an indication of progressive inflammation and arthritis induction. Animals that were not treated saw an increase in paw swelling from +27.69% (0 day) to +234.61% (21 days) and even further up to +163.84% (28 days), indicating arthritis progression. The standard-treated group, on the other hand, showed a significant decrease in paw oedema size, as the extent of inhibition was from -13.51% to -33.65% confirming significant inhibition of arthritic symptoms and inflammatory response. Of all compounds tested, compound 5b showed very high antiarthritic activity which caused a gradual decrease in paw oedema throughout the treatment period. The compound showed -7.42% inhibition on day 0, which gradually increased to -8.33% (7 days), -37.98% (14 days), -42.14% (21 days), and -43.68% (28 days) is depicted in Figure 2. The greatest decrease on day 28 suggests high anti-antiarthritic activity and prevention of arthritis development. In particular, compound 5b showed higher inhibition when paw oedema was measured at later stages (21 and 28 days) in comparison to the control drug indicating high anti-arthritic activity. The continuing decrease in paw swelling could be explained by the inhibition of inflammatory mediators, reduction in the number of immune cells, and regulation of pathways that play a role in chronic arthritis. Hence, the results indicated that compound 5b exhibited promising anti arthritic efficacy, which could be used as starting molecules in the preparing of anti-antiarthritic drugs.

S. No.	Time (h)	% Changes in paw volume		
		Control group	Standard group	Compound 5b
1	0 day	+ 27.69	- 13.51	-7.42
2	7 days	+ 38.46	- 1.38	- 8.33
3	14 days	+ 161.63	- 33.65	-37.98

4	21 days	+ 234.61	- 29.69	- 42.14
5	28 days	+ 163.84	- 27.83	- 43.68

Table 1. % change in paw oedema after treatment.

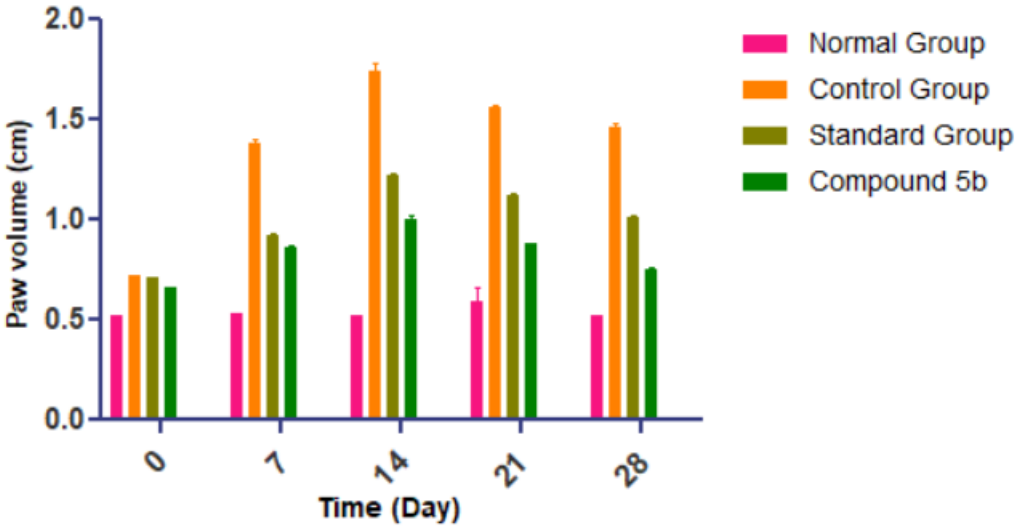

Figure 2. Effect of daidzein on the paw volume in rats

3.3 Computational Study

3.3.1 Molecular Docking Study

Molecular Docking Study

A molecular docking study was conducted to evaluate the binding affinity and interaction pattern of the synthesized quinazoline derivatives (5a-f) with the active site of the target protein, comparing them to the standard drug, Leflunomide. The docking results indicated that all the designed ligands exhibited better binding properties than the standard, as reflected by improved MolDock scores. The synthesized compounds had MolDock score values ranging from -163.360 to -193.269 kcal/mol, while the standard drug scored -122.456 kcal/mol, suggesting a higher capability of the compounds to interact with the protein(Table 1). The stability of complex formation was primarily attributed to hydrogen bonding interactions between compound 5b and key amino acid residues, including Thr212, Asn382, Thr206, Trp387, Gln203,and His388. Similarly, compound 5d displayed significant interactions with residues Thr212, Thr206, Asn382, Trp387, and His388, indicating similar interaction behavior (Figure 3). The drug mostly formed hydrogen bonds with Thr212, Asn382, Thr383, and His388. Notably, all the designed ligands maintained these interactions and also established additional contacts with other residues, such as Gln203, Thr206, Trp387, Gln454, and Ser455, which may enhance binding stability and inhibitory activity. The common interactions with amino acids for both the standard drug and synthesized compounds suggest that they likely share the same binding mode within the active pocket of the target protein. Although compound 5c had the lowest docking score among the two, it formed ten H-bonds with amino acid residues, including Ala199, Gln203, Tyr385, His207, Gln454, Thr212, Thr383, and Ser455. Overall, the docking results demonstrated that the synthesized derivatives possess strong binding potential and form robust intermolecular interactions with the biological target, supporting their potential as inhibitors. The three-dimensional (3D) molecular images of compounds 5b and 5d in the active sites of the target protein are revealed in Figure

4. The docked complexes exhibited favorable binding orientations and maintained good stability within the catalytic pocket. Interactions with key amino acid residues at the active site were observed for both compounds, similar to those with the standard drug, indicating enhanced binding affinity and stability in the docking analysis. Such interactions may suggest higher targeting potential of the synthesized derivatives toward the selected protein.

Compound ID	MolDock Score (kcal/mol)	Interaction (kcal/mol)	H-Bond (kcal/mol)	No. of H-bonds	H-bonds Interaction
Lefluonamide	-122.456	-46.852	-10.85	6	Thr212, Asn382, Thr383, His388
5a	-171.552	-84.779	-12.01	9	Thr212, Asn382, Gln454, Thr383, Ser455
5b	-193.269	-131.075	-13.26	7	Thr212, Asn382, Thr206, Trp387, Gln203, His388
5c	-163.36	-59.386	-3.53	10	Ala199, Gln203, Tyr385, His207, Gln454, Thr212, Thr383, Ser455
5d	-189.469	-124.187	-7.57	6	Thr212, Thr206, Asn382, Trp387, His388
5e	-181.095	-127.481	-6.90	5	Gln203, His388, Trp387, Thr206
5f	-174.503	-39.6520	-11.52	6	Thr212, Thr383, Ser455, Asn382

Table 1. Molecular docking results of synthesized sulfonamide containing Pteridine analogues (5a–f) and the standard drug Leflunomide against the target protein.

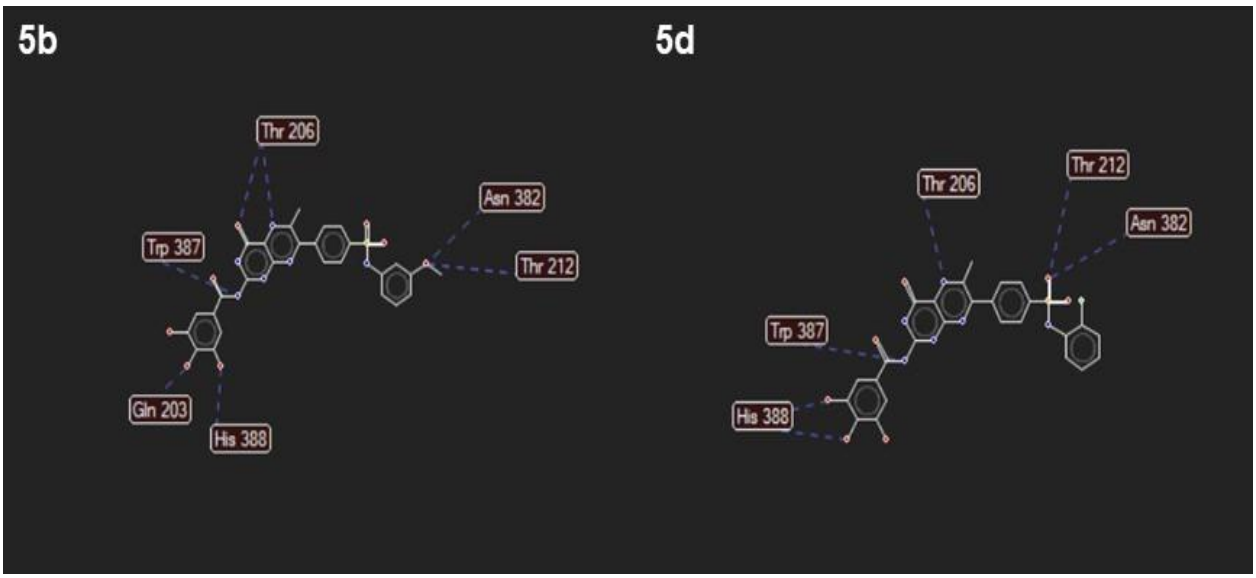

Figure 3. 2D molecular interaction analysis of compounds 5b and 5d within the active binding pocket of the target protein, illustrating hydrogen bonding and hydrophobic interactions with key amino acid residues.

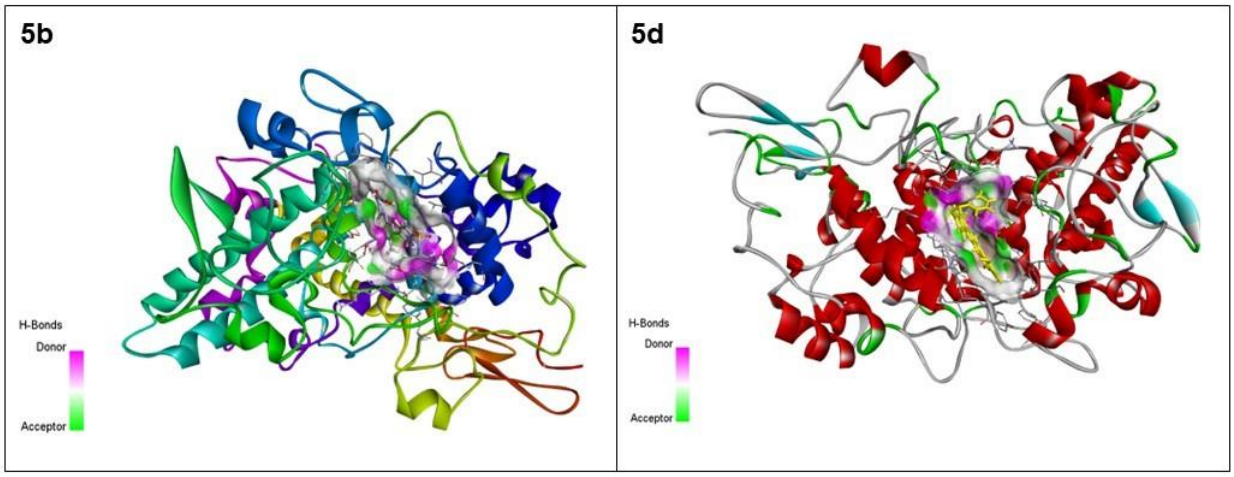

Figure 4. 3D molecular visualization of compounds 5b and 5d docked into the active site of the target protein, showing binding orientation and stabilization within the catalytic pocket.

CONCLUSION

In the present study, a series of novel Sulfonamide conjugates of Pteridines (5a-f) were successfully synthesized and characterized by FT-IR, NMR, and Mass spectral analysis techniques. The synthesized compounds showed good antioxidant and antiarthritic activity in the biological evaluation. Overall, compound 5b showed the highest antioxidant capacity (IC_{50} = 28.77 ± 0.86 µg/mL), best inhibition of paw oedema (-43.68% at the 28th day) for the CFA-induced arthritis model, and best binding affinity in the molecular docking study (MolDock score = -193.269 kcal/mol) with the target protein. The increased activity of 5b could be explained by the structural properties and bio-affinity towards the amino acid residues, which are crucial for the inflammatory pathways. The experimental and computational data support the idea that compound 5b might prove to have anti-arthritic properties and might be a promising lead compound for the preparation of new medicines to treat rheumatoid arthritis. It may be useful for further pharmacological and toxicity studies to confirm its clinical utility and safety.

REFERENCES

1. Hasan AA, Khudhur HR, Hameed AK. Rheumatic autoimmune diseases (focus on RA): prevalence, types, causes, and diagnosis. Karbala Journal of Pharmaceutical Sciences. 2022 Jan 1;1(20).
2. Alivernini S, Firestein GS, McInnes IB. The pathogenesis of rheumatoid arthritis. Immunity. 2022 Dec 13;55(12):2255-70.
3. Cheng Q, Wu H, Du Y. The roles of small-molecule inflammatory mediators in rheumatoid arthritis. Scandinavian journal of immunology. 2021 Mar;93(3):e12982.
4. Leban J, Vitt D. Human dihydroorotate dehydrogenase inhibitors, a novel approach for the treatment of autoimmune and inflammatory diseases. Arzneimittelforschung. 2011 Jan;61(01):66-72.
5. Shamshad H, Bakri R, Mirza AZ. Dihydrofolate reductase, thymidylate synthase, and serine hydroxymethyltransferase: Successful targets against some infectious diseases. Molecular biology reports. 2022 Jul;49(7):6659-91.
6. Sramek M, Neradil J, Veselska R. Much more than you expected: the non-DHFR-mediated effects of methotrexate. Biochimica et Biophysica Acta (BBA)-General Subjects. 2017 Mar 1;1861(3):499-503.
7. El Azab IH, Khalifa ME, Gobouri AA, Altalhi TA. Synthesis, Characterization, and Pharmacological Evaluation of Some New Pteridine-Based Heterocycles as Antimicrobial Agents. Journal of Heterocyclic Chemistry. 2019 Apr;56(4):1352-61.
8. Singh N, Pandey J, Anireddy J. Synthesis, characterization, computational analysis and antimicrobial assay of novel naphthyloxy and naphthylphenoxyderivatives.International journal of scientific & technology research. 2019; 8(10); 2277-8616.
9. Abuelizz HA, El-Dib RA, Marzouk M, Al-Salahi R. In vitro evaluation of new 2-phenoxy-benzo [g] [1, 2, 4] triazolo [1, 5-a] quinazoline derivatives as antimicrobial agents. Microbial pathogenesis. 2018 Apr 1; 117:60-7.
10. N. B. Eddy and D. J. Leimbach, "Synthetic analgesics II. Dithienylbutenyl and dithienylbutylamines," Journal of Pharmacology and ExperimentalTherapeutics, vol. 107, no. 3, pp. 385– 393, 1953.
11. Turan-Zitouni G, Yurttaş L, Kaplancıklı ZA, Can ÖD, DemirÖzkay Ü. Synthesis and anti-nociceptive, anti-inflammatory activities of new aroyl propionic acid derivatives including N-acylhydrazone motif. Medicinal Chemistry Research. 2015 Jun;24(6):2406-16.
12. Rani P, Pal D, Rama R; Hashim S. (2014). Anticancer, Anti-Inflammatory, and Analgesic Activities of Synthesized 2-(Substituted phenoxy) Acetamide Derivatives. BioMed Research International: 2014; 9; 386473.
13. Diment D, Musl O, Balakshin M, Rigo D. Guidelines for Evaluating the Antioxidant Activity of Lignin via the 2, 2-diphenyl-1-picrylhydrazyl (DPPH) Assay. ChemSusChem. 2025 May 19;18(10):e202402383.
14. Newbould BB. Chemotherapy of arthritis induced in rats by Mycobacteria adjuvant. Br J Pharmacol Chemother. 1963 Aug;21(1):127-36.
15. Daharia A, Thakur AS, Dewangan L. A Computational Strategy for Validation of Piperidine as Lead from Phytochemical evaluation for Antiglycation activity via AGEs-RAGE Pathway Modulation. Journal of Pharma Insights and Research. 2025 Dec 5;3(6):273-84.
16. Al-Mijalli SH, Mrabti HN, Elbouzidi A, Ashmawy NS, Batbat A, Abdallah EM, Laaboudi W, Aladhadh M, Alshabrmi FM, Alnasser SM, Addi M. Thymus serpyllum L. Essential Oil: Phytochemistry and in Vitro and in Silico Screening of Its Antimicrobial, Antioxidant and Anti-Inflammatory Properties. Phyton (0031-9457). 2025 Jan 1;94(1).
17. Daharia A, Thakur AS, Dewangan L. Molecular docking, synthesis, and antiglycation activity of novel polyhydroxy-containing pyrrolidine derivatives. Journal of the Iranian Chemical Society. 2026 Mar;23(3):86.
18. Daharia A, Thakur AS, Dewangan L. Microwave-Assisted Synthesis of Some Novel Polyhydroxy Piperidine Compounds for Antiglycation Activity: In-Vitro and In-Silico Validation. Chemistry Africa. 2026 Jan;9(1):15.
19. Dewangan L, Thakur AS, Daharia A. Development of novel sulphonyl chalcone-pyrimidinone derivatives as potent inhibitors of acetylcholinesterase for alzheimer's disease

treatment. Analytical Chemistry Letters. 2026 Jan 2;16(1):28-42.

20. Sakure K, Daharia A, Thakur AS, Pradhan M, Badwaik H. Exploration of Neuroprotective and Retinoprotective Mechanisms of Plumbagin Using Network Pharmacology and Molecular Docking. Journal of Pharma Insights and Research. 2026 Apr 5;4(2):092-101.

HOW TO CITE: Nitypal Singh Chouhan*[1], Hemant Badwaik[2], Design And Synthesis Of Sulfonamides Containing New Pteridine Analogues For The Management Of Rheumatoid Arthritis, Int. J. Sci. R. Tech., 2026, 3 (6), 273-286. https://doi.org/10.5281/zenodo.20538563